ISSN 0018-151X, High Temperature, 2013, Vol. 51, No. 3, pp. 369–376. © Pleiades Publishing, Ltd., 2013.
Original Russian Text © A.E. Galashev, O.R. Rakhmanova, 2013, published in Teplofizika Vysokikh Temperatur, 2013, Vol. 51, No. 3, pp. 412–420.

THERMOPHYSICAL PROPERTIES OF MATERIALS

Computer Study of Methane Adsorption by Water Clusters

A. E. Galashev and O. R. Rakhmanova

Institute of Industrial Ecology, Ural Branch, Russian Academy of Sciences, Yekaterinburg, Russia

Received June 7, 2012

Abstract—Methane adsorption by water clusters including 50 molecules was studied by the molecular dynamics (MD) technique. The calculated frequency dependence of the real and imaginary parts of the dielectric permittivity points to the prevalence of a high-frequency mode in the spectra of these parameters after methane is adsorbed by water clusters. Such changes are also observed in the spectrum of the IR radiation absorption coefficient; however, the average value of this coefficient remains nearly the same. Methane adsorption causes a considerable increase in the reflection coefficient of the disperse water medium and the integrated power of IR radiation emission.

DOI: 10.1134/S0018151X13020065

INTRODUCTION

Gas hydrates are mixtures constituted by inclusions; they can be formed both naturally and synthetically, when water molecules and appropriate guest molecules interact at low temperatures and high pressures. Selectivity of hydrate cells to guest molecules and a gas retaining potential in hydrates is well known [1]. The observed natural hydrates of methane can be considered as a medium in which natural gas is stored [2]. A hydrate can have guest cells of different sizes, which are filled up with various inclusion molecules (sH-hydrate). Methane, along with xenon and carbon dioxide, occupies small cells, forming the sI-hydrate [3]. However, at extremely high pressures, methane can also occupy large cells of the sH-hydrate with their multiple occupation [4]. Guest molecules in hydrates have a low affinity to water; therefore, there are three separate phases in the system: a gas, a nonaqueous liquid of the included molecules, and a water component. All of the molecules are in intimate contact with each other and can form the sH-hydrate under suitable conditions. At present, the reason for different occupation of guest cells with methane is not perfectly clear.

Methane clathrates are stable in the permafrost at a depth of greater than 200 m and in pelagic sediments deeper than 250 m under the condition that the ocean floor is rather cold. The thickness of the zone where clathrates are stable depends on the temperature of the ocean surface and the temperature gradient profile. Methane concentration with respect to water in the stability zone determines whether the clathrates would appear or not. A low depth of the stability zone makes clathrates susceptible to disturbances at the ocean surface. Warming of the continental shelf caused by rising tides in the ocean and changes in pressure with depth, for instance, due to a fall in the sea level, destabilizes clathrates in the ocean, while growth of icebergs stabilizes clathrates situated below them. The time scale of thermal stabilization is determined by the thermal properties of the sediments and is on the order of thousands of years [5]. The time required to include methane in clathrates due to cooling from the ocean surface takes several tens of thousands of years. The sensitivity of clathrates to changes at the ocean surface depends on the time scale of clathrate formation; therefore, a great amount of carbon remains in the form of clathrates. This points to the fact that clathrates can play an important role in changes in the atmosphere composition and influence the properties of glacial drifts.

Up to now, primary attention was paid to study of the properties of extensive methane clathrates, and there are only a few works on investigation of the cluster hydrophobic effect in the atmosphere [6–8]. Under atmospheric conditions, the pressure effect needed for methane hydrates to be formed diminishes. The greater the pressure, the higher the temperature at which methane hydrate is stable. Thus, at 273 K, it is stable at ~2.5 MPa and greater. Such pressures are attainable, for instance, at a depth of 250 m in the ocean. At atmospheric pressure, a temperature of about 193°C is needed for the methane hydrate to be stable. Methane hydrates can be stable under low pressures even at higher temperatures, because they become covered with an ice crust under decomposition, which hinders their further decay. To elucidate the physical properties of methane hydrates, investigation at the molecular level is needed, which can be carried out using the molecular dynamics technique. For example, in [9–11], the spectral properties of a disperse water medium that adsorbed ozone, including cases when bromine and nitrates ions were present, were calculated.

The aim of the present study was to investigate the optical effect arising due to methane adsorption by large water clusters, which manifests itself in changes

in spectra of the radiation absorption coefficient, IR radiation emission, and IR radiation reflection.

MOLECULAR DYNAMICS MODEL

The interaction between water molecules in clusters was described by a nonadditive potential whose additive part is the modified [12] TIP4P potential of water [13] and the nonadditive part is specified by the polarization interaction; therefore, the total energy of the system is given by the formula

$$U_{\text{tot}} = U_{\text{pair}} + U_{\text{pol}},$$

where the pair term of the potential energy is determined by Lennard-Jones and Coulomb contributions

$$U_{\text{pair}} = \sum_i \sum_j \left[4\varepsilon^{(\text{LJ})} \left\{ \left(\frac{\sigma_{ij}^{(\text{LJ})}}{r_{ij}} \right)^{12} - \left(\frac{\sigma_{ij}^{(\text{LJ})}}{r_{ij}} \right)^{6} \right\} + \frac{q_i q_j}{r_{ij}} \right].$$

Here r_{ij} is the distance between atoms i and j, q is the electric charge, and $\sigma^{(\text{LJ})}$ and $\varepsilon^{(\text{LJ})}$ are the parameters of the Lennard-Jones potential [12].

The polarization energy is determined as

$$U_{\text{pol}} = -\frac{1}{2} \sum_i \mathbf{d}_i \cdot \mathbf{E}_i^0,$$

where $\mathbf{E}_i^0$ is the strength of the field induced by the system of fixed charges at the point determining localization of the molecule i:

$$\mathbf{E}_i^0 = \sum_{j \neq i} \frac{q_j \mathbf{r}_{ij}}{r_{ij}^3};$$

and $\mathbf{d}_i$ is the induced dipole moment assigned to this molecule:

$$\mathbf{d}_i = \alpha_i^p \mathbf{E}_i,$$

where

$$\mathbf{E}_i = \mathbf{E}_i^0 + \sum_{j \neq i} \hat{\mathbf{T}}_{ij} \cdot \mathbf{d}_j.$$

Here $\mathbf{E}_i$ is the strength of the total electric field at the point determining the molecule i in the polarization interaction, α_i^p is the molecular polarizability, and $\hat{\mathbf{T}}_{ij}$ is the tensor of dipole–dipole interaction

$$\hat{\mathbf{T}}_{ij} = \frac{1}{|r_{ij}|^3} (3\mathbf{u}_{ij}\mathbf{u}_{ij} - \hat{\mathbf{1}}),$$

where $\mathbf{u}_{ij}$ is a unit vector in the direction of $\mathbf{r}_i - \mathbf{r}_j$; $\mathbf{r}_i$ and $\mathbf{r}_j$ are vectors determining the position of the polarization-active points i and j of the corresponding molecules, and $\hat{\mathbf{1}}$ is a 3×3 unit tensor.

On the basis of work [12], we suppose that the value of the permanent dipole moment for the water molecule is the same as its experimental value 1.848 D. The geometry of the H_2O molecule corresponds to its experimental parameters in the gaseous phase: $r_{\text{OH}} = 0.09572$ nm and the H–O–H angle is 104.5° [14]. Fixed charges ($q_{\text{H}} = 0.519e$ and $q_M = -1.038e$) are assigned to H atoms and the point M lying on the bisector of the H–O–H angle at a 0.0215-nm distance from the oxygen atom. The values of charges and the position of the point M are chosen so as to reproduce experimental values of the dipole and quadrupole moments [15, 16] and the ab initio calculated energy of a dimer and typical distances in it [17]. Stabilization of the short-range order in water clusters is achieved largely due to the short-range Lennard-Jones potential with the center of interaction related to the oxygen atom. In addition to the electrical charge, polarizability needed for the description of the nonadditive polarization energy is also referred to the point M. At each time step, a standard iterative procedure is used to calculate the induced dipole moments $\mathbf{d}_i$ [12]. The accuracy of $\mathbf{d}_i$ determination is within 10^{-5}–10^{-4} D.

Atom–atomic methane–methane interactions were specified by Mie–Lennard-Jones and Coulomb contributions

$$\Phi_{ij}(r) = \varepsilon_{ij} \left[\left(\frac{r_0}{r_{ij}} \right)^{12} - 2 \left(\frac{r_0}{r_{ij}} \right)^{6} \right] + \frac{q_i q_j}{r_{ij}}.$$

The values of the parameters ε_{ij}, r_0, and q_i for atoms H and C of the CH_4 molecule were taken as 0.038 kcal/mol, 0.28525 nm, and $0.119e$; and 0.07382 kcal/mol, 0.43 nm, and $-0.476e$, respectively [18]. The parameters of the Lennard-Jones potential describing methane–water interactions were determined using the Berthelot–Lorentz formulas

$$\varepsilon_{aw}^{(\text{LJ})} = \sqrt{\varepsilon_a^{(\text{LJ})} \varepsilon_w^{(\text{LJ})}}, \quad \sigma_{aw}^{(\text{LJ})} = \frac{\sigma_a^{(\text{LJ})} + \sigma_w^{(\text{LJ})}}{2},$$

where $\varepsilon_a^{(\text{LJ})}$ and $\varepsilon_w^{(\text{LJ})}$ are the energetic parameters and $\sigma_a^{(\text{LJ})}$, and $\sigma_w^{(\text{LJ})}$ are the geometric parameters of the potential for the C and H atoms of methane molecules and the O atom of water molecules, respectively [6].

The methane molecule is tetrahedral with a carbon atom in the center and hydrogen atoms at the vertices. The H–C–H angle takes the value of a tetrahedral angle 109°. The distances between atoms in the CH_4 molecule are $r_{\text{CH}} = 0.109$ nm and $r_{\text{HH}} = 0.177$ nm. A nonpolar CH_4 molecule has a greater polarizability α^p (2.6 Å^3), than a water molecule (1.49 Å^3) [19].

The trajectories of centers of mass of molecules were determined by the Gear fourth-order method [20]. The time integration step Δt was 0.2×10^{-16} s. At first, in the MD calculations with a duration of $2 \times 10^6 \Delta t$, the equilibrium condition was established for pure water clusters with no impurity inclusions at $T = 233$ K. The configuration of the $(H_2O)_{50}$ cluster corresponding to the time point of 40 ps was used further as the initial configuration for simulation of heteroclusters $(CH_4)_i(H_2O)_{50}$, $1 \leq i \leq 6$. Each of the attached CH_4 molecules was initially positioned so that the distance

between the atoms of this molecule and the atoms of water molecules was about 0.6 nm. The centers of mass of CH_4 molecules were initially placed at the coordinate axes outside the water cluster. The initial orientation of water molecules was arbitrary. Balancing of the newly formed cluster was carried out in the time interval $1.2 \times 10^6 \Delta t$ at $T = 233$ K, and then, in the time interval of $5 \times 10^6 \Delta t$ at the same temperature, the appropriate physico-chemical properties were calculated. The system of $(CH_4)_i(H_2O)_{50}$ clusters was formed according to the statistical weights of clusters established in the following way. Let us consider the case of nonpolarized light scattering when the free path l of molecules is much shorter than the wavelength λ. The extinction (attenuation) coefficient h of the incident beam is determined, on the one hand, by the Rayleigh equation [21], and, on the other hand, by the scattering coefficient ρ ($h = \frac{16\pi}{3}\rho$) [22] in the assumption of scattering at an angle of 90°. Taking into account that $h = \alpha + \rho$, where α is the absorption coefficient, we have

$$N = \frac{2\omega^4}{3\pi c^4}\frac{(\sqrt{\varepsilon}-1)^2}{\alpha}\left(1-\frac{3}{16\pi}\right).$$

Here N is the number of scattering centers per 1 cm^3, c is the light velocity, ε is the dielectric permittivity, and ω is the frequency of the incident wave.

Let us denote the following types of superdispersed systems as monodisperse system I of $(H_2O)_{50}$ clusters, region II filled with water clusters of 10 to 50 molecules in size (the number of molecules in a cluster increases at a step of $\Delta n = 5$); and medium III composed of $(H_2O)_{50}$ clusters which adsorbed one to six CH_4 molecules.

Let us compose systems II and III out of $(H_2O)_n$ and $(CH_4)_i(H_2O)_{50}$ clusters, respectively, so a cluster containing i impurity molecules and n water molecules has a statistical weight of

$$W_{in} = \frac{N_{in}}{N_{l\Sigma}}, 1 \le i \le 6,\ 10 \le n \le 50\ (\Delta_n = 5),$$

where N_{in} is the number of clusters with n water molecules and i CH_4 molecules per 1 cm^3, and the index l takes the values 1 and 2: $N_{1\Sigma} = \sum_{n=1}^{9} N_{i=0,n}$ and $N_{2\Sigma} = \sum_{i=1}^{6} N_{i,n=50}$. Further calculations were performed taking into account the assumed statistical weights W_{in}.

The analytical solution of motion equations for molecular rotation was accomplished using the Rodrigues–Hamilton parameters [23]; and the integration scheme of motion equations considering rotations corresponded to the approach proposed by Sonnenschein [24].

DIELECTRIC PROPERTIES

The total dipole moment of a cluster $\mathbf{d}_{cl}$ was calculated by the equation

$$\mathbf{d}_{cl}(t) = Z_+ \sum_{i=1}^{N_{tot1}} \mathbf{r}_i(t) + Z_- \sum_{j=1}^{N_{tot2}} \mathbf{r}_j(t),$$

where $\mathbf{r}_i(t)$ is a vector pointing to the position of atom i or point M at the moment t; Z is the electric charge in the considered center; the sign + is assigned to positively charged H atoms, and the sign – is assigned to the point M or to C atoms; and N_{tot1} and N_{tot2} are the numbers of positively and negatively charged atoms in a cluster, respectively.

The static dielectric constant ε_0 was calculated using fluctuations of the total dipole moment $\mathbf{d}_{cl}$ [25]:

$$\varepsilon_0 = 1 + \frac{4\pi}{3VkT}\left[\left\langle \mathbf{d}_{cl}^2 \right\rangle - \left\langle \mathbf{d}_{cl} \right\rangle^2\right],$$

where V is the cluster volume and k is the Boltzmann constant.

Dielectric permittivity $\varepsilon(\omega)$ as a function of frequency ω was represented by the complex value $\varepsilon(\omega) = \varepsilon'(\omega) - i\varepsilon''(\omega)$, which was calculated by the equation [25, 26]

$$\frac{\varepsilon(\omega)-1}{\varepsilon_0 - 1} = -\int_0^\infty \exp(-i\omega t)\frac{dF}{dt}dt$$

$$= 1 - i\omega\int_0^\infty \exp(-i\omega t)F(t)dt,$$

where $F(t)$ is the normalized autocorrelation function of the total dipole moment of a cluster:

$$F(t) = \frac{\left\langle \mathbf{d}_{cl}(t)\cdot\mathbf{d}_{cl}(0)\right\rangle}{\left\langle \mathbf{d}_{cl}^2\right\rangle}.$$

The outer IR radiation absorption coefficient α can be represented as the imaginary part of the frequency-dependent dielectric permittivity $\varepsilon(\omega)$ in the form [26]

$$\alpha(\omega) = 2\frac{\omega}{c}\mathrm{Im}[\varepsilon(\omega)^{1/2}].$$

The reflection coefficient R is defined as the ratio between the average energy flux reflected from the surface and the incident flux. At normal incidence of a plane monochromatic wave, the reflection coefficient is described by the formula [10, 21]

$$R = \left|\frac{\sqrt{|\varepsilon_1|}-\sqrt{|\varepsilon_2|}}{\sqrt{|\varepsilon_1|}+\sqrt{|\varepsilon_2|}}\right|^2. \quad (1)$$

The frequency dispersion of the dielectric permittivity determines the frequency dependence of the dielectric losses $P(\omega)$ according to the relation [22]

$$P = \frac{\varepsilon''\left\langle E^2\right\rangle\omega}{4\pi},$$

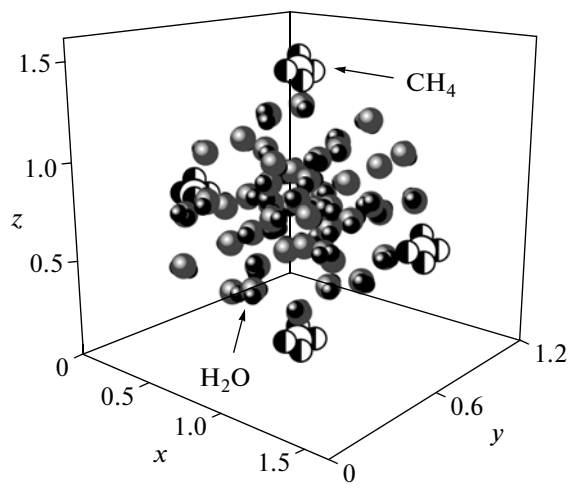

Fig. 1. Configuration of the cluster $(CH_4)_4(H_2O)_{50}$ corresponding to the time of 50 ps.

where $\langle E^2 \rangle$ is the average value of the squared electric field strength and ω is the frequency of the emitted electromagnetic wave.

Motions at a frequency less than 1200 cm^{-1} correspond to molecule librations, and those at frequencies greater than 1200 cm^{-1} describe mainly intramolecular vibrations [27] realized under the following assumption. Flexible models of molecules were considered. Molecule flexibility was achieved using the procedure devised within the framework of the Hamiltonian dynamics in [28, 29]. Let us consider the case of a diatomic molecule. Let atoms a and b be separated by the distance

$$Q = \|\mathbf{r}_a - \mathbf{r}_b\|,$$

where $\mathbf{r}_a$ and $\mathbf{r}_b$ are the vectors determining the positions of atoms. We denote the corresponding velocities by $\mathbf{v}_a$ and $\mathbf{v}_b$, and the reduced mass is defined as

$$\mu = \frac{m_a m_b}{m_a + m_b}.$$

The size of a molecule represented by atoms a and b is determined by equalizing the total potential force $\mathbf{f}(\mathbf{Q}) = -\frac{\partial \mathbf{r}}{\partial \mathbf{Q}} \nabla \Phi(\mathbf{r})$ and the centrifugal force $-\mu Q\omega^2$; thus,

$$-\mu Q\omega^2 - \mathbf{f}(\mathbf{r}) \frac{\partial \mathbf{r}}{\partial \mathbf{Q}} = 0,$$

where $\omega = \|\mathbf{v}_a - \mathbf{v}_b\|/Q$ is the angular velocity. From the condition of the minimum of the contribution from each generalized coordinate to the potential energy U, we obtain

$$\frac{\partial}{\partial Q_i} H(\mathbf{r}, \mathbf{v}) = \frac{\partial}{\partial Q_i} \left(\frac{1}{2} \mu_i Q_i^2 \omega_i^2 + U(\mathbf{r}) \right) = 0.$$

This method is generalized to molecules of any composition [30].

RESULTS OF CALCULATION

Adsorption of i methane molecules by a water cluster results in formation of a cluster $(CH_4)_i(H_2O)_{50}$. The configuration of the cluster $(CH_4)_4(H_2O)_{50}$ including four CH_4 molecules (at the time of 50 ps) is shown in Fig. 1 as an example. Methane molecules are arranged symmetrically relative to the center of the cluster in vertical and horizontal directions. Their orientation is quite random and depends on the position and orientation of the neighboring water molecules. Since the tetrahedral CH_4 molecule carries positive electric charges (belonging to H atoms) on the outside, the tetrahedron vertex is located closer to the negatively charged oxygen atom of the nearest water molecule. Situations in which H atoms of a methane molecule are located near O atoms of two or even three H_2O molecules are also possible. The symmetrical arrangement of hydrophobic methane molecules leads to compaction of the water component of the cluster, which affects its optical properties.

The frequency spectrum of the real and imaginary parts of the dielectric permittivity considerably transforms after CH_4 molecules are adsorbed by water clusters (Fig. 2). While, for the system of identical water clusters (system I) or water clusters with different sizes (system II), the functions $\varepsilon'(\omega)$ and $\varepsilon''(\omega)$ increase rapidly at the beginning of the frequency range (below 1100 cm^{-1}), these functions grow nonmonotonically, achieving the maximal value in the vicinity of the frequencies 3280 and 3070 cm^{-1}, respectively, for the system of $(H_2O)_{50}$ clusters with CH_4 molecules (system III). The largest increase of the $\varepsilon'(\omega)$ function begins at a frequency of 2875 cm^{-1}; and that of the $\varepsilon''(\omega)$ function, at 2500 cm^{-1}. The maximal values of these functions for system III are greater than those for systems I and II. The $\varepsilon'(\omega)$ function calculated in [31] for bulk liquid water decreases nonmonotonically in the frequency range of $200 \le \omega \le 3500$ cm^{-1}, whereas the experimental $\varepsilon''(\omega)$ function [32] undergoes a nonmonotonic drop down to a frequency of ~930 cm^{-1}, at which it becomes monotonic.

Adsorption of CH_4 molecules by water clusters brings about a considerable change in the shape of the spectrum of the IR absorption coefficient (Fig. 3). In this case, the α coefficient rises up to the frequency of 3311 cm^{-1}, at which it takes the absolute maximum. Below 1340 cm^{-1}, the α value for systems I and II is greater than that for system III. However, over the entire frequency range $0 \le \omega \le 3500$ cm^{-1}, the integrated intensity of the $\alpha(\omega)$ spectrum for system III is higher than that for systems I and II by a factor of 1.04 and 1.3, respectively. The principal maxima of the $\alpha(\omega)$ spectra for systems I and III undergo red shifts by 162 and 92 cm^{-1}, respectively, relative to the principal maximum (at a frequency of 3403 cm^{-1}) of the IR absorption spectrum for liquid water [33], while the position of the maximum for system II features a blue shift by 115 cm^{-1} relative to the frequency of 3403 cm^{-1}.

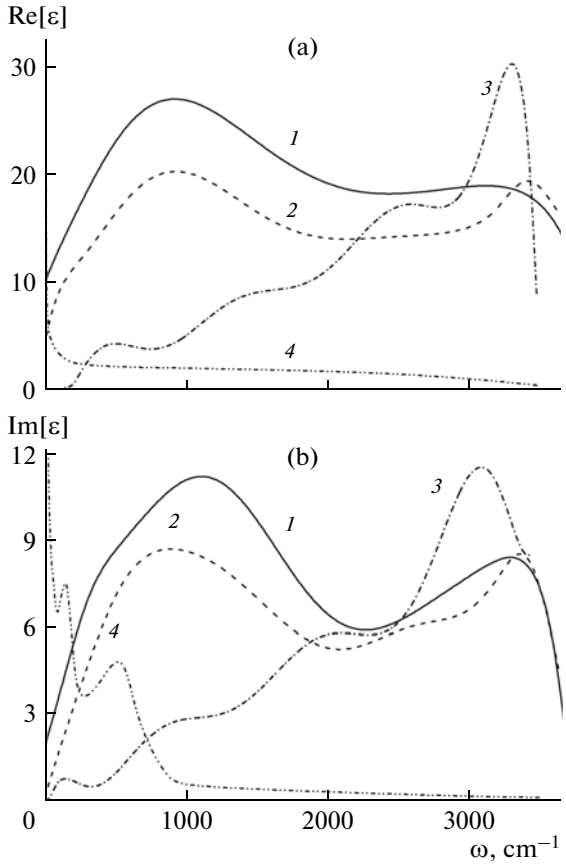

Fig. 2. (a) Real and (b) imaginary parts of the dielectric permittivity for the cluster systems: (*1*) I $(H_2O)_{n=50}$, (*2*) II $(H_2O)_{n=10,\ ...,\ 50}$, (*3*) III $(CH_4)_{i=1,\ ...,\ 6}(H_2O)_{50}$, and (*4*) liquid water; (a) MD calculations [31] and (b) experiment [32].

The spectrum of the IR absorption coefficient of gaseous methane is determined by two well-resolved broad bands at 1325 and 3035 cm^{-1} [34, 35]. The inset in Fig. 3 shows the experimental IR spectrum of a solid mixture H_2O/CH_4 at a temperature of 15 K. The main well-resolved peaks at 750, 1600, 2200, and 3250 cm^{-1} are due to the water component of the mixture, and sharp low-intense maxima at 1302 and 3009 cm^{-1} are due to the contribution from methane [36]. Note that the peaks arising due to the water part of the solid system mainly correspond to the positions of peaks in the $\alpha(\omega)$ spectrum of liquid water.

The intensities of individual IR radiation absorption spectra vary over a wide range (Fig. 4), although they all have a similar shape, which differs noticeably from the shape of the $\alpha(\omega)$ spectrum of the $(H_2O)_{50}$ cluster. Only clusters that adsorbed one I_α and six CH_4 molecules have a greater integrated intensity I_α of the $\alpha(\omega)$ spectrum (by a factor of 1.06 and 1.17, respectively), compared to the same value for a pure water cluster. Among the clusters with the integrated intensity I_α of the $\alpha(\omega)$ spectrum smaller than that of the same spectrum for the $(H_2O)_{50}$ cluster, the cluster that absorbed three CH_4 molecules stands out. The I_α value for it is lower than that for the $(H_2O)_{50}$ cluster by a factor of 2.27. The clusters with two, four, and five meth-

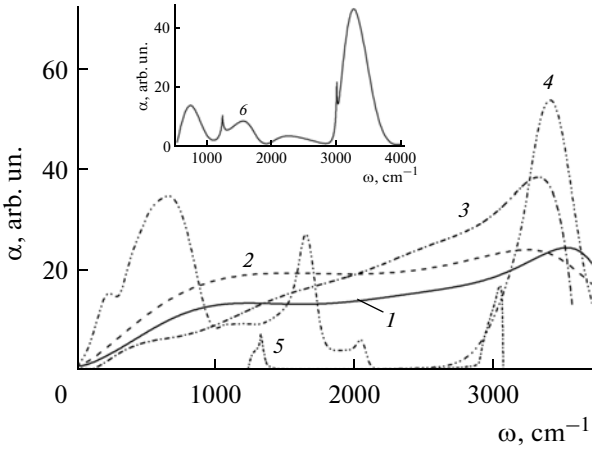

Fig. 3. Absorption coefficient for the cluster systems: (*1*) I, (*2*) II, (*3*) III, and (*4*) experimental $\alpha(\omega)$ function of bulk liquid water [33], (*5*) experimental spectrum for gaseous CH_4 [34, 35], and (*6*) (inset) experimental IR spectrum of a solid mixture H_2O/CH_4 at a temperature of 15 K [36].

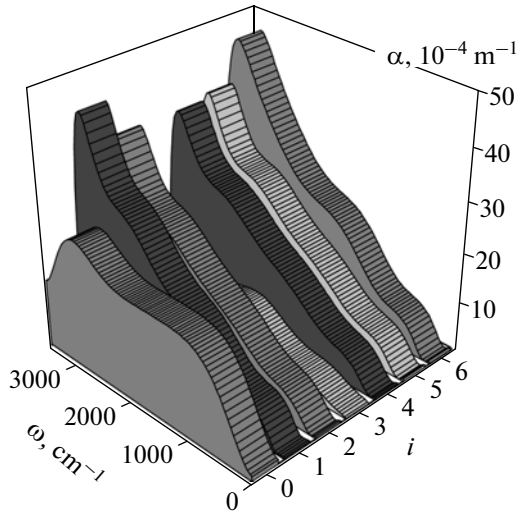

Fig. 4. IR absorption spectra for the clusters $(CH_4)_i(H_2O)_{50}$, $0 \le i \le 6$.

ane molecules have the I_α value lower than that for the pure water cluster by factors of 1.04 to 1.05. The principal peaks of the $\alpha(\omega)$ spectra of the $(CH_4)_i(H_2O)_{50}$ clusters occur at 3307 cm^{-1} except for the cluster with $i = 3$ whose principal maximum is at $\omega = 3349$ cm^{-1}.

The spectrum of reflection of a plane monochromatic electromagnetic wave shows that, for water clusters that adsorbed methane, IR radiation is reflected more intensely (Fig. 5). While the IR radiation reflection coefficient averaged over frequency $\bar{R}$ for systems I and II was 0.41 and 0.35, respectively, its value for system III achieved as high as 0.74. Note that, in all of the cases considered, the $R(\omega)$ spectrum is continuous. After CH_4 molecules are adsorbed by clusters, the irregularity of the upper boundary of the $R(\omega)$ spectrum rises in addition to an increase in the integrated intensity. The position of the maximum of the $R(\omega)$ spectrum shifted from 1014 to 3254 cm^{-1} due to capture of methane molecules by water clusters.

The reflection spectra of a plane wave for individual clusters in the form of an approximation by polynomials of the ninth degree are presented in Fig. 6. We see that, once a single CH_4 molecule is adsorbed, the shape and intensity of the $R(\omega)$ spectrum change drastically. In addition, all $R(\omega)$ spectra for water clusters which captured CH_4 molecules are alike in shape and differ by intensity. The cluster containing three methane molecules has the lowest integrated intensity I_R of the $R(\omega)$ spectrum. However, even in this case, the I_R value is 0.75% higher than the same characteristic of the $R(\omega)$ spectrum for the $(H_2O)_{50}$ cluster. Except for the case of $i = 3$, with a growing number of CH_4 molecules successively attached to the water cluster, the I_R

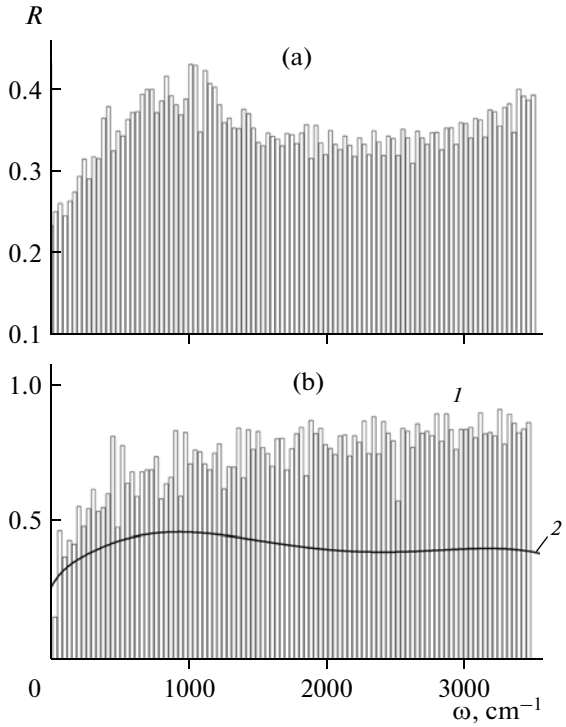

Fig. 5. Coefficient of reflection of a plane monochromatic electromagnetic wave by the disperse systems (a) II and (b) (*1*) I and (*2*) III.

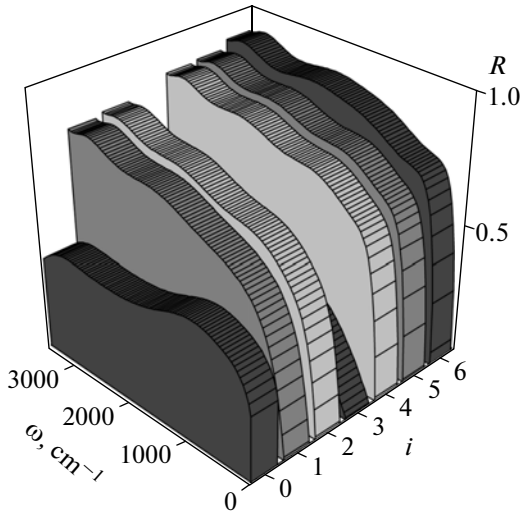

Fig. 6. Coefficient of reflection of a normally incident plane monochromatic electromagnetic wave from the surface of the clusters $(CH_4)_i(H_2O)_{50}$, $0 \le i \le 6$.

value rises and becomes greater than the same characteristic for the pure water cluster by factors of 1.57 and 1.93 at $i = 1$ and 6, respectively.

The radiation source power shows how quickly the intensity of the radiation changes. The radiation power density of scattering particles determines the "visibility" of these radiators. The intensity of the IR radiation emission spectra of clusters changes considerably after CH_4 molecules are adsorbed by water clusters (Fig. 7). The integrated intensity I_P of the $P(\omega)$ spectrum for system III rises by a factor of 1.68 as compared to the same characteristic for system I and by a factor of 2.16 as compared to the same characteristic for system II. The maximum of the $P(\omega)$ spectrum for system III occurs at a frequency of 3105 cm^{-1}, while the maxima for systems I and II occur at 3340 and 3500 cm^{-1}. The positions of the main emission bands in the $P(\omega)$ spectra for systems III and I are shifted toward lower frequencies by 206 and 102 cm^{-1} relative to the most intense bands in the corresponding $\alpha(\omega)$ IR radiation absorption spectra. In this case, emission is not accompanied by additional photon absorption. In the case of system II, the difference between the main frequencies of emission and absorption is negative ($\Delta\omega = -20$ cm^{-1}); therefore, the emission process needs additional photons to be absorbed. However, since the $\Delta\omega$ value is small, we can suppose that resonance emission takes place.

The individual $P(\omega)$ spectra of $(CH_4)_i(H_2O)_{50}$ clusters are alike in shape (Fig. 8). However, they differ drastically in integrated intensity. The I_P value of the $P(\omega)$ spectrum for the cluster with $i = 6$ is greater than that for the cluster with $i = 3$ by a factor of 8.26. After one to three CH_4 molecules are attached to the water cluster, the I_P value decreases (by a factor of up to 4.68), and, after four or six methane molecules are captured by a water cluster, the I_P value rises (by a fac-

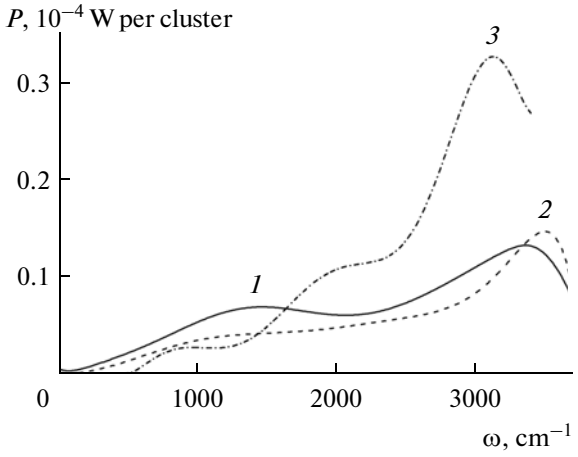

Fig. 7. IR radiation emission spectra for the systems (*1*) I, (*2*) II, and (*3*) III.

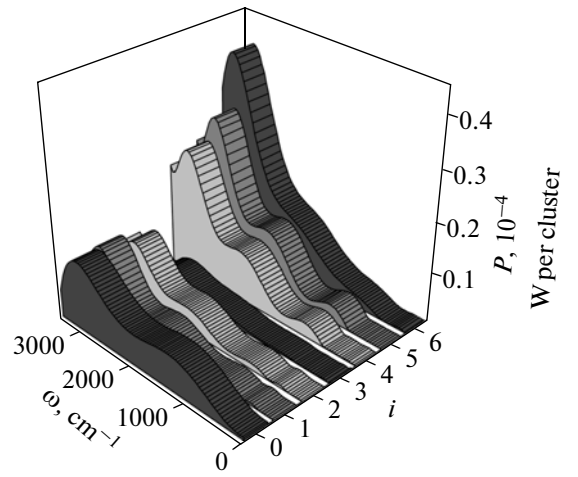

Fig. 8. IR radiation emission spectra for the clusters $(CH_4)_i(H_2O)_{50}$, $0 \le i \le 6$.

tor of no greater than 1.76). The position of the principal peak in the $P(\omega)$ spectra of the clusters changes from 2761 (at $i = 3$) to 3055 cm^{-1} (at $i = 2, 4, 5$). At $i = 6$, the principal peak is located at a greater frequency (3181 cm^{-1}) than at $i = 1$ (3139 cm^{-1}).

CONCLUSIONS

Liberation of methane and its subsequent oxidation to carbon dioxide can be responsible for the observed variations in the concentration of atmospheric methane and carbon dioxide during formation of glaciers. Since methane and carbon dioxide are strong absorbents of IR radiation, liberation and capture of methane by clathrates contributes to the mechanisms of strong feedback to "radiation forcing", affecting the Earth's climate, which takes place due to orbital changes in the Earth.

Therefore, there is a link between the increase in methane concentration and the increase in moisture content in the atmosphere. Herein, we strived to answer how optical properties of a disperse water medium change due to methane adsorption. Calculations established that the maxima of the spectra of the real and imaginary parts of dielectric permittivity shift toward higher frequencies. The average coefficient of IR radiation absorption determined in the substantially important frequency range of the equilibrium emission of the Earth does not change considerably due to methane adsorption; however, its spectra transform, with its intensity increasing in the high-frequency range. Methane adsorption results in a considerable increase in the average reflection coefficient of the plane monochromatic electromagnetic wave and a change in the shape of the frequency reflection spectrum. After methane was adsorbed, the velocity of IR radiation emission of the disperse water medium increases heavily, and the average radiation power becomes about two times greater. The behavior of the main radiation processes is rather strongly dependent upon the concentration of methane captured by the disperse water medium. This dependence becomes more apparent in the case of IR radiation emission, in which, starting from a certain concentration value, the integrated emission intensity rises steadily.

REFERENCES

1. Koh, C.A. and Sloan, E.D., *AIChE J.*, 2007, vol. 53, p. 1636.
2. Ehglezos, P. and Lee, J.D., *Korean J. Chem. Eng.*, 2005, vol. 22, p. 671.
3. Loveday, J.S., Nelmes, R.J., Guthrie, M., Belmote, S.A., Allan, D.R., Klug, D.D., Tse, J.S., and Handa, Y.P.M., *Nature* (London), 2001, vol. 410, p. 661.
4. Loveday, J.S., Nelmes, R.J., Klug, D.D., Tse, J.S., and Desgreniers, S., *Can. J. Phys.*, 2003, vol. 81, p. 539.
5. MacDonald, G.J., *Clim. Change*, 1990, vol. 16, p. 247.
6. Galashev, A.Y., *Mol. Simul.*, 2010, vol. 36, p. 273.
7. Galashev, A.E., Chukanov, V.N., Novruzov, A.N., and Novruzova, O.A., *High Temp.*, 2006, vol. 44, no. 3, p. 364.
8. Galashev, A.E., Novruzov, A.N., and Galasheva, A.A., *Khim. Fiz.*, 2006, vol. 25, no. 2, p. 26.
9. Galashev, A.E., Rakhmanova, O.R., and Novruzova, O.A., *High Temp.*, 2011, vol. 49, no. 2, p. 193.
10. Galashev, A.E., Rakhmanova, O.R., and Novruzova, O.A., *High Temp.*, 2011, vol. 49, no. 4, p. 528.
11. Galashev, A.E., *High Temp.*, 2012, vol. 50, no. 2, p. 204.
12. Dang, L.X. and Chang, T.-M., *J. Chem. Phys.*, 1997, vol. 106, p. 8149.
13. Jorgensen, W.L. and Madura, J.D., *J. Am. Chem. Soc.*, 1983, vol. 105, p. 1407.
14. Benedict, W.S., Gailar, N., and Plyler, E.K., *J. Chem. Phys.*, 1956, vol. 24, p. 1139.
15. Xantheas, S., *J. Chem. Phys.*, 1996, vol. 104, p. 8821.
16. Feller, D. and Dixon, D.A., *J. Chem. Phys.*, 1996, vol. 100, p. 2993.
17. Smith, D.E. and Dang, L.X., *J. Chem. Phys.,* 1994, vol. 100, p. 3757.
18. New, M.H. and Berne, B.J., *J. Am. Chem. Soc.*, 1995, vol. 117, p. 7172.
19. *Spravochnik khimika* (A Reference Book of Chemist), Nikol'skii, B.P., Ed., Leningrad: Khimiya, 1971, vol. 1.
20. Haile, J.M., *Molecular Dynamics Simulation: Elementary Methods*, New York: John Wiley and Sons, 1992.
21. Landau, L.D. and Lifshitz, E.M., *Course of Theoretical Physics*, Volume 8: *Electrodynamics of Continuous Media*, Oxford: Butterworth–Heinemann, 1984.
22. *Fizicheskaya entsiklopediya* (Physical Encyclopedia), Prokhorov, A.M., Ed., Moscow: Sovetskaya Entsiklopediya, 1988, vol. 1, p. 702.
23. Koshlyakov, V.N., *Zadachi dinamiki tverdogo tela i prikladnoi teorii giroskopov* (Problems in the Dynamics of the Solid State and in the Applied Theory of Gyroscopes), Moscow: Nauka, 1985.
24. Sonnenschein, R., *J. Comput. Phys.*, 1985, vol. 59, p. 347.
25. Bresme, F., *J. Chem. Phys.*, 2001, vol. 115, p. 7564.
26. Neumann, M., *J. Chem. Phys.*, 1985, vol. 82, p. 5663.
27. Stern, H.A. and Berne, B.J., *J. Chem. Phys.*, 2001, vol. 115, p. 7622.
28. Lemberg, H.L. and Stillinger, F.H., *J. Chem. Phys.*, 1975, vol. 62, p. 1677.
29. Rahman, A., Stillinger, F.H., and Lemberg, H.L., *J. Chem. Phys.*, 1975, vol. 63, p. 5223.
30. Saint-Martin, H., Hess, B., and Berendsen, H.J.C., *J. Chem. Phys.*, 2004, vol. 120, p. 11133.
31. Neumann, M., *J. Chem. Phys.*, 1986, vol. 85, p. 1567.
32. Angell, C.A. and Rodgers, V., *J. Chem. Phys.*, 1984, vol. 80, p. 6245.
33. Goggin, P.L. and Carr, C., in *Water and Aqueous Solutions,* Neilson, G.W. and Enderby, J.E., Eds., Bristol (United Kingdom): Adam Hilger, 1986, vol. 37, p. 149.
34. Toth, R.A., Brown, L.R., Hunt, R.H., and Rothman, L.S., *Appl. Opt.*, 1981, vol. 20, p. 932.
35. Albert, S., Bauerecker, A., Boudon, V., Brown, L.R., Champion, J.-P., Löete, M., Nikitin, A., and Quack, M., *Chem. Phys.*, 2009, vol. 356, p. 131.
36. Bernstein, M.P., Cruikshank, D.P., and Sandford, S.A., *Icarus*, 2006, vol. 181, p. 302.